Preprint typeset in JHEP style - PAPER VERSION NORDITA-2010-102, RH-27-2010

Holographic metals at finite temperature

V. Giangreco M. Puletti,[1)] **S. Nowling,**[1)] **L. Thorlacius,**[1),2)] **and T. Zingg**[1),2)]

1) NORDITA, Roslagstullsbacken 23
SE-106 91 Stockholm, Sweden

2) University of Iceland, Science Institute
Dunhaga 3, IS-107 Reykjavik, Iceland

E-mail: valentina, nowling, larus, zingg @nordita.org

Abstract: A holographic dual description of a 2+1 dimensional system of strongly interacting fermions at low temperature and finite charge density is given in terms of an electron cloud suspended over the horizon of a charged black hole in asymptotically AdS spacetime. The electron star of Hartnoll and Tavanfar is recovered in the limit of zero temperature, while at higher temperatures the fraction of charge carried by the electron cloud is reduced and at a critical temperature there is a third order phase transition to a configuration with only a charged black hole. The geometric structure implies that finite temperature transport coefficients, including the AC electrical conductivity, only receive contributions from bulk fermions within a finite band in the radial direction.

Keywords: Field Theories in Lower Dimensions, Quantum Critical Points, Gauge-gravity correspondence, Black Holes.

Contents

1. Introduction

There has been considerable recent interest in developing holographic models of strongly coupled physics in low dimensions with a view towards condensed matter systems (see [1, 2, 3, 4] for reviews). This can be motivated both from the point of view of extending the gauge theory/gravity correspondence to include a variety of interesting field theoretic systems without supersymmetry, and also from the point of view of gaining a new theoretical handle on materials containing strongly correlated electrons.

In a recent paper Hartnoll and Tavanfar [5] considered a simple holographic model for strongly interacting fermions in 2+1 dimensions at zero temperature and finite charge density. In their approach, which builds on earlier work in [6, 7], the bulk Maxwell field, which is dual to the field theory current, is sourced by an ideal fluid consisting of charged free fermions. The combined Einstein, Maxwell, and fluid field equations in the bulk spacetime have planar solutions, referred to as electron stars in [5], where the charge and energy densities of the bulk fermion fluid have a non-trivial radial profile. The geometry is asymptotically AdS but deep in the electron star interior the metric exhibits Lifshitz scaling with a non-universal dynamical critical exponent that depends on the couplings of the model. Similar constructions were considered in [8, 9] for neutral and charged free fermion fluids supported by a degeneracy pressure.

In the present paper we extend the gravity dual description of [5] to include finite temperature configurations in the boundary field theory. We construct static solutions of the bulk field equations where an 'electron cloud' is suspended above the horizon of a charged black hole, or more precisely a black brane with a planar

horizon. The electron cloud has both an outer and an inner edge. The outer edge is also found in the electron stars of [5] but the inner edge is a new feature, found only at finite temperature. At the inner edge the gravitational pull of the black brane on the electron fluid is balanced by electrostatic repulsion.

In the fluid description, observables in the boundary theory, such as the electric conductivity, only receive contributions from bulk fermions located within a band of finite width in the radial direction. The sharpness of the edges is presumably an artifact of the classical perfect fluid description and we expect both quantum corrections and fluid interactions to give rise to tails in the bulk fermion profile that fall off towards the boundary and the black brane horizon, respectively.[1]

At the level of classical geometry, a finite temperature in the boundary theory is introduced by including a black hole in the bulk spacetime, with a non-vanishing Hawking temperature. Quantum effects in the bulk include thermal Hawking radiation, which comes to equilibrium with the bulk fermion fluid, but at weak gravitational coupling this thermalization in the bulk is suppressed and will not be considered here. This simplifies our analysis considerably as it allows us to use a zero temperature equation of state for the free fermions in the bulk to capture finite temperature effects in the boundary field theory.

At low temperatures in the boundary theory, the electric charge in the bulk geometry is partly carried by the electron cloud and partly by the charged black brane inside it. As the temperature is raised, the two edges of the electron cloud move towards each other and an ever larger fraction of the total electric charge in the bulk geometry resides inside the black brane. The two edges of the electron fluid meet at a finite critical temperature, above which there is only a black brane solution with no electron cloud present. We find that the system undergoes a third order phase transition at the critical point.[2]

As the temperature is lowered, on the other hand, the inner edge of the electron cloud approaches the black brane horizon, which in turn recedes towards vanishing area. In the zero temperature limit, one recovers the electron star geometry where there is no longer any black hole and all the charge is carried by the electron fluid. We confirm this by showing that the horizon recedes from the boundary, the geometry at low temperature encodes the dynamical exponent z, and by comparing free energy densities. We find that at low temperatures the free energy density of an electron cloud geometry smoothly goes over to that of an electron star. Furthermore, we compare the free energy densities between an electron cloud solution and an AdS-RN black brane solution at finite temperature. We find that, whenever a solution with an electron cloud exists, it is favored over an AdS-RN black brane.

[1] Such tails are, for instance, found in an alternative approach to including bulk fermions based on a single fermion wave equation [11].

[2] In an earlier version of the paper it was incorrectly stated that the phase transition was second order. The correct behavior was identified in [10].

The electrical conductivity at finite temperature can be obtained for this system using, by now, standard holographic techniques (see for instance [1, 2]). We find that the finite temperature conductivity smoothly interpolates between the AdS-RN and electron star results [5].

The same finite temperature solutions were found independently by Hartnoll and Petrov in [10]. Initially there was a discrepancy between their work and ours in the analysis of the phase transition, but after correcting an error in our expression for the free energy density, we now also find a third order phase transition.

2. Field equations and electron cloud solutions

The Einstein-Maxwell equations with a negative cosmological constant and a charged perfect fluid are

$$R_{\mu\nu} - \frac{1}{2} g_{\mu\nu} R - \frac{3}{L^2} g_{\mu\nu} = \kappa^2 (T^{\text{Maxwell}}_{\mu\nu} + T^{\text{fluid}}_{\mu\nu}) \,, \qquad \nabla^\nu F_{\mu\nu} = e^2 \, J^{\text{fluid}}_\mu \,. \tag{2.1}$$

We adopt units where the characteristic AdS length scale is $L = 1$. The source terms are given by

$$T^{\text{Maxwell}}_{\mu\nu} = \frac{1}{e^2} (F_{\mu\lambda} F_\nu{}^\lambda - \frac{1}{4} g_{\mu\nu} F_{\lambda\sigma} F_\nu^{\lambda\sigma}) \,, \tag{2.2}$$

$$T^{\text{fluid}}_{\mu\nu} = (\rho + p) u_\mu u_\nu + p \, g_{\mu\nu} \,, \tag{2.3}$$

$$J^{\text{fluid}}_\mu = \sigma u_\mu \,, \tag{2.4}$$

where σ is the charge density of the fluid, ρ is its energy density, p the pressure, and u^μ the four velocity, $u^\mu u_\mu = -1$. The justification and limitations of the perfect fluid description are discussed in detail in [5] and the same considerations apply here.

We look for static black brane solutions with planar symmetry,

$$ds^2 = -f(v) dt^2 + g(v) dv^2 + \frac{1}{v^2} (dx^2 + dy^2) \,, \qquad A = \frac{e}{\kappa} h(v) \, dt \,, \tag{2.5}$$

where the radial coordinate goes from $v \to 0$ at the asymptotic boundary to a constant value $v = v_0$ at the black brane horizon. We find it convenient to introduce a scale invariant variable $u = -\log(v/v_0)$, such that $u = 0$ at the horizon and $u \to \infty$ at the boundary, and work with rescaled fields,

$$\hat{f} = v_0^2 f, \quad \hat{g} = v_0^2 g, \quad \hat{h} = v_0 h, \quad \hat{p} = \kappa^2 p, \quad \hat{\rho} = \kappa^2 \rho, \quad \hat{\sigma} = e \kappa \sigma \,. \tag{2.6}$$

The equations of motion (2.1) can then be expressed in a first order form, convenient

for numerical evaluation,

$$\frac{d\hat{f}}{du}+\frac{\hat{k}^2}{2}+\hat{f}(1-3e^{-2u}\hat{g})=e^{-2u}\hat{f}\hat{g}\hat{p}\,, \tag{2.7}$$

$$\frac{d\hat{k}}{du}+\hat{k}=e^{-2u}\left(\frac{1}{2}\hat{h}\hat{k}+\hat{f}\right)\frac{\hat{g}\hat{\sigma}}{\sqrt{\hat{f}}}\,, \tag{2.8}$$

$$\frac{1}{\hat{f}}\frac{d\hat{f}}{du}+\frac{1}{\hat{g}}\frac{d\hat{g}}{du}-4=e^{-2u}\frac{\hat{g}\hat{h}\hat{\sigma}}{\sqrt{\hat{f}}}\,, \tag{2.9}$$

where $\hat{k}\equiv d\hat{h}/du$. Following [5], we assume a free fermion equation of state defined via

$$\hat{\sigma}=\hat{\beta}\int_{\hat{m}}^{\hat{\mu}}d\varepsilon\,\varepsilon\sqrt{\varepsilon^2-\hat{m}^2}\,,\qquad \hat{\rho}=\hat{\beta}\int_{\hat{m}}^{\hat{\mu}}d\varepsilon\,\varepsilon^2\sqrt{\varepsilon^2-\hat{m}^2}\,,\qquad -\hat{p}=\hat{\rho}-\hat{\mu}\hat{\sigma}\,, \tag{2.10}$$

where $\hat{\beta}$ is a coupling dependent dimensionless constant, $\hat{m}$ is proportional to the electron mass, $\hat{m}^2=\frac{\kappa^2}{e^2}m^2$, and the (rescaled) local chemical potential $\hat{\mu}$ is given by the background Maxwell gauge field in the tangent frame, $\hat{\mu}\equiv\hat{h}/\sqrt{\hat{f}}$.

As discussed in [5], there is a range of parameters,

$$e^2\sim\frac{\kappa}{L}\ll 1\,, \tag{2.11}$$

for which we can assume a classical bulk geometry with a non-trivial back-reaction due to the fermion fluid. If, at the same time, the Compton wavelength of the fermions is small compared to the AdS length scale,

$$mL\gg 1\,, \tag{2.12}$$

then we are also justified in taking spacetime to be locally flat in the fermion equation of state. These conditions amount to the dimensionless parameters in the equation of state (2.10) taking order one values [5],

$$\hat{\beta}\sim 1\,,\qquad \hat{m}^2\sim 1\,. \tag{2.13}$$

The construction of the electron cloud geometry proceeds in a few steps. First we solve the vacuum equations, with $\hat{\sigma}=\hat{\rho}=\hat{p}=0$, to find the charged AdS-RN black brane solution inside the cloud,

$$\hat{f}=e^{2u}+\frac{\hat{q}^2}{2}e^{-2u}-(1+\frac{\hat{q}^2}{2})e^{-u}\,,\qquad \hat{g}=\frac{e^{4u}}{\hat{f}}\,,\qquad \hat{h}=\hat{q}(1-e^{-u})\,. \tag{2.14}$$

The dimensionless constant $\hat{q}$ is proportional to the charge carried by the black brane and we have used the freedom to rescale the time coordinate t to fix the

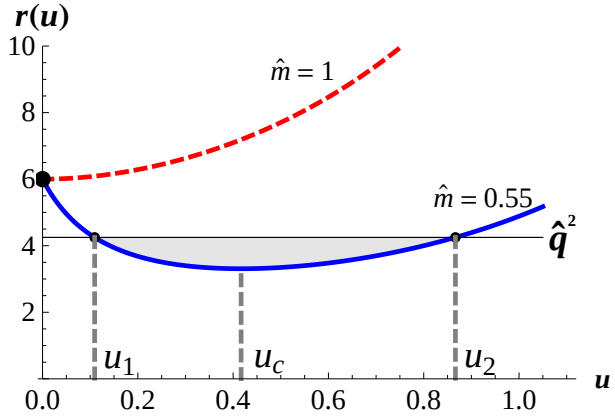

Figure 1: The auxilliary function $r(u)$ in (2.16), used in the construction of the electron cloud solution, is plotted for $\hat{m} = 1$ (dashed red) and $\hat{m} = 0.55$ (solid blue).

overall normalization of $\hat{f}$. When the charge parameter is in the range $\hat{q}^2 < 6$ the black brane is non-extremal with a non-degenerate horizon, where the local chemical potential $\hat{\mu}$ vanishes. As we move away from the horizon the chemical potential grows but remains too small to support a fermion fluid until,

$$\hat{\mu}^2 = \frac{\hat{h}^2(u)}{\hat{f}(u)} > \hat{m}^2 \,. \tag{2.15}$$

We will only consider non-vanishing fermion mass. For zero fermion mass the inner edge of the electron cloud reaches the horizon for all temperatures. The geometry, with the back-reaction from the fermion fluid included, is then harder to determine and we will not consider this case here.

The condition (2.15) is easily seen to be equivalent to

$$\hat{q}^2 > \frac{\hat{m}^2 e^u (e^{2u} + e^u + 1)}{e^u - 1 + \frac{\hat{m}^2}{2}} \equiv r(u) \,. \tag{2.16}$$

The right hand side is shown for two different values of $\hat{m}^2$ in Figure 1. It can be read off from the figure that:

- There cannot be any fermion fluid outside a non-extremal black brane if $\hat{m}^2 \geq 1$, since in this case $r(u) > 6$ for all $u > 0$. This restriction on $\hat{m}$ was already seen in [5] as a condition for the existence of electron star solutions at zero temperature.

- For $\hat{m}^2 < 1$ and a near-extremal black brane with $\hat{q}^2 < 6$, the condition (2.16) is satisfied within a finite interval $u_1 < u < u_2$, indicated in the figure. The endpoints of the interval correspond the inner and outer edges of the electron cloud in a 'probe' approximation, where the back-reaction on the geometry due to the fermion fluid is ignored.

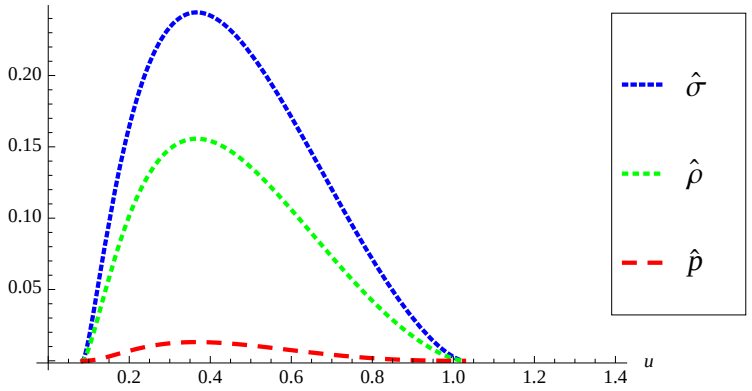

Figure 2: The radial profiles of the fluid variables $(\hat{\sigma}, \hat{\rho}, \hat{p})$ for $\hat{m} = 0.55$, $\hat{\beta} = 10$, and $\hat{q}^2 = 4.49$.

- For $\hat{m}^2 < 1$ and $\hat{q}^2$ below a critical value (which depends on $\hat{m}^2$), the condition (2.16) is not satisfied for any $u > 0$. This implies there is a critical temperature above which there is only a black brane and no electron fluid in the bulk.

The second step in the construction of an electron cloud solution with back-reaction included is to numerically integrate the field equations (2.7) - (2.9) starting from the inner edge of the electron cloud. The functions $\hat{f}$, $\hat{g}$, $\hat{h}$, and $\hat{k}$ are continuous at the matching point $u = u_1$ and thus we can generate initial values for the numerical integration using the exact AdS-RN solution (2.14) with $\hat{q}$ determined from (2.16) evaluated at $u = u_1$.

The local chemical potential $\hat{\mu}$ goes to zero in the asymptotic $u \to \infty$ region and the numerical integration is terminated at a point $u = u_s$ where the condition (2.16) is no longer satisfied. We find that the back-reaction of the fermion fluid on the geometry leads to $u_s > u_2$, and that this effect becomes more pronounced, $u_s \gg u_2$, at low temperature. Figure 2 shows numerical results for the fluid variables $\hat{\sigma}$, $\hat{\rho}$, and $\hat{p}$ for $\hat{m} = 0.55$, $\hat{\beta} = 10$, and $\hat{q}^2 = 4.49$.

The third and final step in the construction is to obtain the spacetime geometry outside the electron cloud by matching the numerical solution onto a charged black brane solution at $u = u_s$ in much the same way as is done for electron stars in [5]. The exterior solution has the general form

$$\hat{f} = c_s^2 e^{2u} + \frac{Q_s^2}{2} e^{-2u} - M_s e^{-u}\,, \qquad \hat{g} = \frac{c_s^2 e^{4u}}{\hat{f}}\,, \qquad \hat{h} = \mu_s - Q_s e^{-u}\,, \tag{2.17}$$

where the subscript s denotes on the various constant parameters is a reminder that they are determined by matching onto a numerical solution at $u = u_s$. We already fixed the overall scale of the time coordinate when writing the inside black brane solution in (2.14) so now there appears an extra parameter c_s in $\hat{f}$. Also, since the

external solution only extends to $u = u_s$ and not to an event horizon, we do not require the usual relationship between M_s, Q_s, and μ_s found for a vacuum AdS-RN black brane. The parameters in (2.17) are instead determined to be

$$c_s^2 = \hat{f}(u_s)\hat{g}(u_s)e^{-4u_s}\,, \tag{2.18}$$

$$Q_s = \hat{k}(u_s)e^{u_s}\,, \tag{2.19}$$

$$\mu_s = \hat{h}(u_s) + \hat{k}(u_s)\,, \tag{2.20}$$

$$M_s = \hat{f}(u_s)\hat{g}(u_s)e^{-u_s} + \frac{1}{2}\hat{k}^2(u_s)e^{u_s} - \hat{f}(u_s)e^{u_s}\,. \tag{2.21}$$

These parameters refer to the rescaled fields in (2.6) while the physical parameters appearing in an external AdS-RN solution with a canonically normalized time coordinate are given by

$$\mu = \frac{\mu_s}{c_s v_0}\,, \qquad Q = \frac{Q_s}{c_s v_0^2}\,, \qquad M = \frac{M_s}{c_s^2 v_0^3}\,. \tag{2.22}$$

Once the parameters of the external black brane solution have been determined for given values of $\hat{m}$, $\hat{\beta}$, and $\hat{q}$, standard methods can be used to obtain the free energy density as a function of temperature for these geometries. This will be carried out in Section 3 below.

The next step is to determine the Hawking temperature of the electron cloud geometry, which is to be identified with the temperature in the boundary field theory. The Hawking temperature is easily obtained from the behavior of the Euclidean metric near the horizon. One finds

$$\frac{T}{\mu} = \frac{6 - \hat{q}^2}{8\pi\mu_s}\,, \tag{2.23}$$

where we have again divided by the physical chemical potential μ in order to have a dimensionless quantity to work with.

In the limit of zero temperature we expect to recover the electron star geometry of [5]. In this case the radial coordinate extends to $u \to -\infty$ and the metric exhibits Lifshitz scaling in the deep interior.

In Figure 3 one can see that the curvature scalar R as a function of the proper distance s measured from the outside of the electron cloud is approaching the expected asymptotic value for a Lifshitz geometry as we lower the temperature T before plunging to $R = -12$ at the horizon. From R evaluated on the solution and the metric, one confirms the correct dynamical exponent, e.g. $z = 5.75466$ when $\hat{m} = .55$ and $\hat{\beta} = 10$.

On the left in Figure 4, we see that the horizon radius vanishes as the temperature is lowered indicating that the horizon recedes from the AdS boundary. Furthermore by fitting the low temperature data in the figure, we find that

$$\frac{T}{\mu} \propto \left(\frac{1}{\mu v_0}\right)^z\,, \tag{2.24}$$

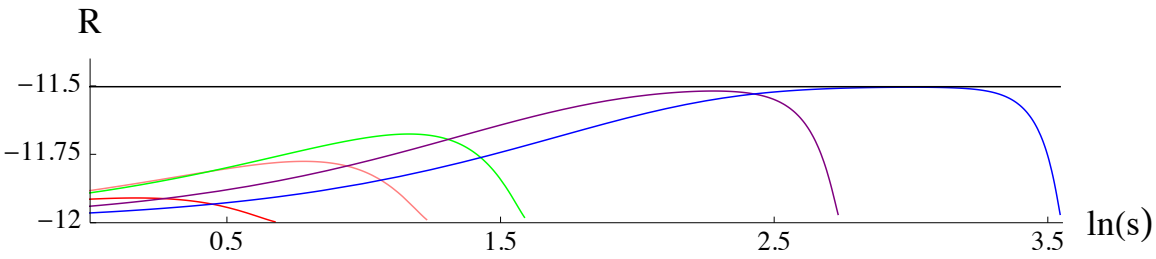

Figure 3: The curvature scalar R versus the proper distance s measured from the outer edge of the electron cloud for $\hat{m} = .55\,, \hat{\beta} = 10$ and for T/μ values $.55, .22, 9.4\times10^{-2}, 9\times10^{-4}$ and 1×10^{-5}. The curves extend further to the right with decreasing temperature. The value for R in the Lifshitz region deep inside an electron star with the same $\hat{m}$ and $\hat{\beta}$ is shown as a horizontal line for reference.

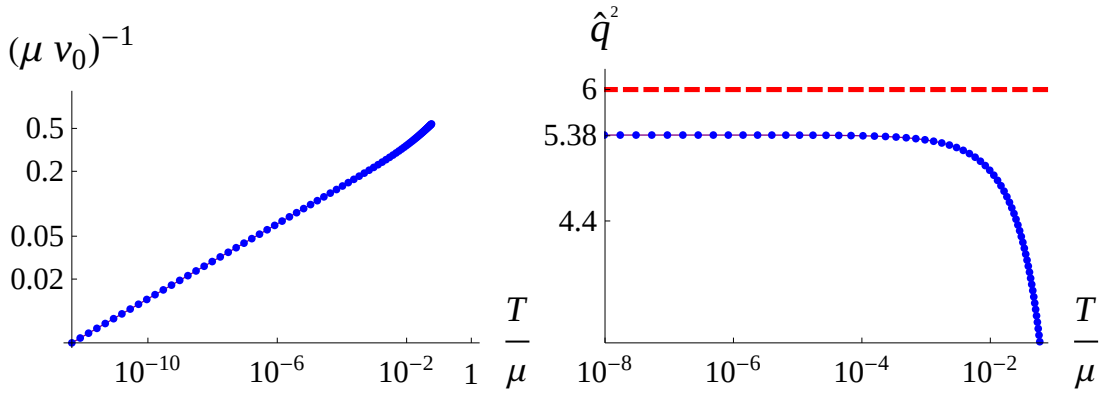

Figure 4: On the left we plot the horizon radius v_0^{-1} as a function of the temperature, T. On the right we show the charge parameter of the inside black brane solution (2.14), $\hat{q}^2$, versus T for $\hat{m} = .55$ and $\hat{\beta} = 10$. For reference we plot the extremal value $\hat{q}^2 = 6$.

where z matches the appropriate expected Lifshitz exponent to a very high precision. This is further evidence that the anisotropic scaling found inside the electron star is recovered by our electron cloud solutions at low temperature.

The plot on the right in Figure 4 shows that the zero temperature limit in the boundary theory is in fact not obtained by approaching an extremal interior black brane, which would have $\hat{q}^2 = 6$. This is at first sight counterintuitive but can ultimately be traced to the focusing effect that the electron fluid has on the geometry outside the black brane. If one were to try to construct an electron cloud solution starting with a value of $\hat{q}^2$ that is closer to 6, than what is seen in the figure the metric would collapse to a curvature singularity at a finite proper distance outside the horizon and the solution would never reach an asymptotic AdS region.

3. Free energy

Further evidence that the electron cloud solution is the proper finite temperature extension of an electron star comes from comparing free energy densities. We obtain the free energy by evaluating the on-shell Euclidean action of the bulk system, including the usual Gibbons-Hawking boundary term [12] and boundary counterterms required for regularization [13, 14]. A bulk action for the charged electron fluid also needs to be included, as described in [5]. The full bulk action turns out to be the integral of a total derivative, and when combined with the appropriate boundary terms, it gives a simple result for the free energy density,

$$F = M - \mu\, Q \, - sT\,, \tag{3.1}$$

where s is the Bekenstein-Hawking entropy density.[3] This can be simplified by using the thermodynamic relation

$$\frac{3}{2}M - \mu\, Q - s\, T = 0\,, \tag{3.2}$$

giving

$$F = -\frac{M}{2}\,. \tag{3.3}$$

The relation (3.1) follows from the radial conservation of the quantity

$$D = \frac{e^{3u}}{\sqrt{\hat{f}\hat{g}}}\left(-2\hat{h}\hat{k} - 2\hat{f} + \frac{d\hat{f}}{du}\right)\,. \tag{3.4}$$

By using the equations of motion (2.7) - (2.10), it is straightforward to check that $\frac{dD}{du} = 0$ and one then evaluates D at the horizon and at the $u \to \infty$ boundary to obtain (3.2).

Using (2.22), the free energy density can be re-expressed in terms of output parameters from our numerical evaluation,

$$F = -\frac{1}{2}\frac{M_s}{c_s^2 v_0^3}\,. \tag{3.5}$$

The factor of v_0^3 in the denominator tells us that we should instead work with the dimensionless quantity

$$\frac{F}{\mu^3} = -\frac{1}{2}\frac{c_s M_s}{\mu_s^3}\,, \tag{3.6}$$

when comparing free energy densities.

In Figure 5 we use these dimensionless variables to compare the free energy densities of various geometries for a typical case when $\hat{m} = .55$ and $\hat{\beta} = 10$, holding

[3] In an earlier version of the paper the sT term was missing from the expression for the free energy density. This led to an incorrect characterization of the phase transition.

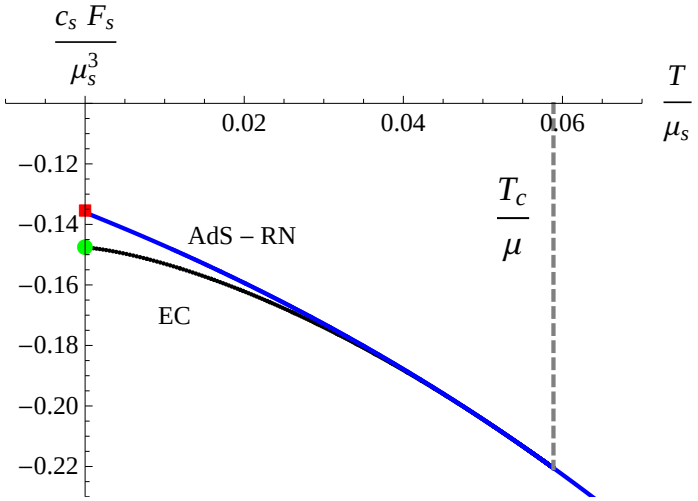

Figure 5: The free energy densities of AdS-RN black brane and electron cloud solutions for $\hat{\beta} = 10$ and $\hat{m} = .55$. In addition the free energy for an extremal black hole and the electron star solution of [5] are shown with a red box and a green dot, respectively.

the chemical potential fixed. One readily sees that the electron cloud solution is preferred over the black brane solution up to the point where the local chemical potential is too low to support any fluid. Beyond this point the only solution is an AdS-RN black brane. At low temperatures, on the other hand, the free energy density of the electron cloud geometries approaches that of the corresponding electron star.

In addition to the low-temperature regime, it is also interesting to ask about the nature of the transition to the AdS-RN black brane solution at higher temperatures. To address this issue, we consider the difference in energy densities between an electron cloud solution just below the critical temperature T_c and an AdS-RN black brane solution,

$$\Delta\left(\frac{F}{\mu^3}\right) \equiv \left(\frac{F}{\mu^3}\right)_{AdS-RN} - \left(\frac{F}{\mu^3}\right)_{EC}, \tag{3.7}$$

at the same value of T/μ. Figure 6 show a log-log plot of this difference near the critical point where one loses the cloud solution at $T_c/\mu = 0.058868$ for $\hat{m} = .55$ and $\hat{\beta} = 10$. The solid curve in Figure 6 is a straight line of slope 3 giving numerical evidence of a third order phase transition where

$$\Delta\left(\frac{F}{\mu^3}\right) = \mathcal{O}\left(\frac{T_c - T}{\mu}\right)^3. \tag{3.8}$$

This feature was observed numerically in [10], and those authors also gave a simple analytic argument for this behavior.

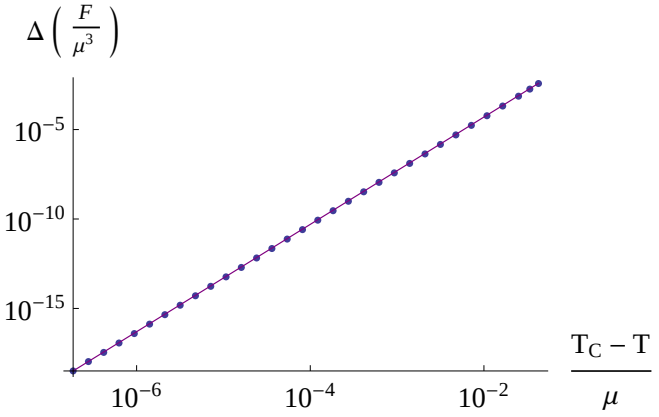

Figure 6: The difference between the black brane and electron cloud free energies near the phase transition temperature at $\hat{\beta} = 10$ and $\hat{m} = .55$.

4. Electric conductivity

The finite temperature AC conductivity at zero momentum can be computed in an analogous way as was done for the zero temperature electron star in [5]. In fact, the finite temperature computation is more standard since in this case the ingoing boundary conditions [15] for the fluctuations in the gauge field are imposed at a smooth black brane horizon rather than at the (mildly) singular Lifshitz horizon inside an electron star.

The background is perturbed, assuming a time dependence of the form $e^{-i\omega t}$, and the resulting equations are linearized. To get a closed system of equations, the following perturbations are needed

$$\hat{A}_x = \delta\hat{A}_x(u)e^{-i\omega t}\,, \qquad \hat{g}_{tx} = \delta\hat{g}_{tx}(u)e^{-i\omega t}\,, \qquad \hat{u}_x = \delta\hat{u}_x(u)e^{-i\omega t}. \tag{4.1}$$

This leads to a system of four first order differential equations

$$\delta\hat{A}_x + \frac{\hat{h}}{\hat{f}}\,\delta\hat{g}_{tx} + e^{2u}\hat{\mu}\,\delta\hat{u}_x = 0, \tag{4.2}$$

$$\frac{d\delta\hat{g}_{tx}}{du} - 2\delta\hat{g}_{tx} + 2\,\frac{d\hat{h}}{du}\,\delta\hat{A}_x = 0, \tag{4.3}$$

$$e^u\frac{d\delta\hat{A}_x}{du} + \sqrt{\frac{\hat{g}}{\hat{f}}}\delta\hat{B}_x = 0, \tag{4.4}$$

$$e^u\,\frac{d\delta\hat{B}_x}{du} + \left[\frac{1}{\sqrt{\hat{f}\hat{g}}}\left(2e^{2u}\frac{d\hat{h}}{du}^2 - \omega_s^2\hat{g}\right) + \frac{\hat{f}\hat{\sigma}\sqrt{\hat{g}}}{\hat{h}}\right]\delta\hat{A}_x = 0, \tag{4.5}$$

where ω_s is defined in terms of the canonical normalized frequency ω as $\omega_s = c_s\,v_0\,\omega$. Equation (4.4) can be regarded as the definition of the auxiliary function $\delta\hat{B}_x$. We note that (4.4) and (4.5) form a closed system involving only $\delta\hat{A}_x$ and $\delta\hat{B}_x$.

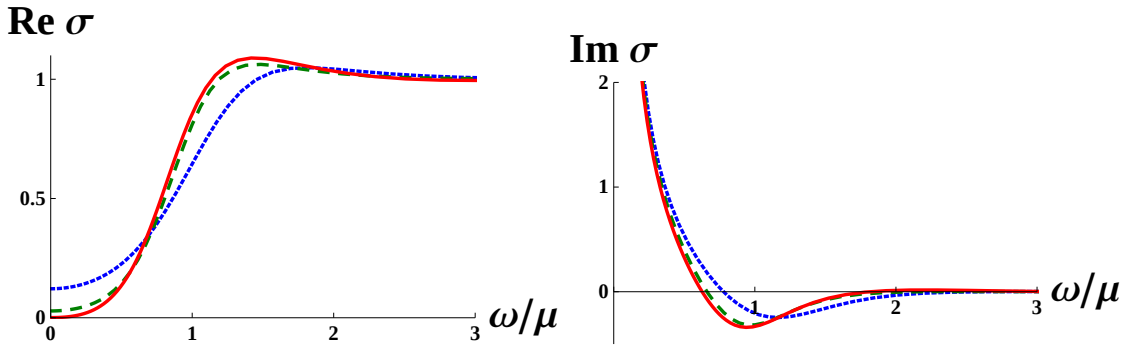

Figure 7: Real and Imaginary part of the conductivity for $\hat{m} = 0.55, \hat{\beta} = 10$. The curves dashed blue, green and solid red correspond to temperature value $T/T_C = 2, 1$ and 0.162, respectively. $T_C = 0.05887$ denotes the critical temperature where the phase transition occurrs. Curves for lower values of T are almost indistinguishable from the one already plottet.

At the horizon, ingoing boundary conditions are imposed [15]. This implies $\delta\hat{A}_x \to u^{-\frac{i\omega}{4\pi T}}$ and $\delta\hat{B}_x \to i\omega u^{-\frac{i\omega}{4\pi T}}$ as $u \to 0$ and T being the Hawking temperature of the AdS-RN black brane solution (2.14). At the AdS boundary, where the background is of the form (2.17), the behavior of those functions is

$$\delta\hat{A}_x = \hat{A}_x^{(0)} + \hat{A}_x^{(1)} e^{-u} + \cdots , \tag{4.6}$$

$$\delta\hat{B}_x = \hat{B}_x^{(0)} + \hat{B}_x^{(1)} e^{-u} + \cdots . \tag{4.7}$$

The coefficients $\hat{A}_x^{(i)}$ and $\hat{B}_x^{(i)}$ are connected, *e.g.* $\hat{B}_x^{(0)} = c_s \hat{A}_x^{(1)}$. This relation can be used to express the conductivity as

$$\sigma = -\frac{i}{\omega_s} \frac{\hat{B}_x^{(0)}}{\hat{A}_x^{(0)}} , \tag{4.8}$$

which is manifestly invariant under the rescaling described in the previous sections.

Our results for the conductivity are obtained by numerics. This is achieved by integrating out from the horizon in the background of an AdS-RN solution, as already indicated, until the inner edge of the electron shell is reached. There, $\delta\hat{A}_x$ and $\delta\hat{B}_x$ need to be continued smoothly into a solution of (4.4) and (4.5) with the electron cloud solution as background. At the outer edge, a second matching to the exterior solution must occur. Finally, the coefficients $\hat{A}_x^{(0)}$ and $\hat{B}_x^{(0)}$ can be read off at the boundary and plugged in to (4.8).

A plot of the conductivity can be seen in Figure 7. The pole in the imaginary part, as usual, indicates the presence of a delta peak in the real part. The offset in the conductivity goes rather quickly to zero once the electron cloud is in place. This is also shown in Figure 8. Parameterizing the real and imaginary part of the

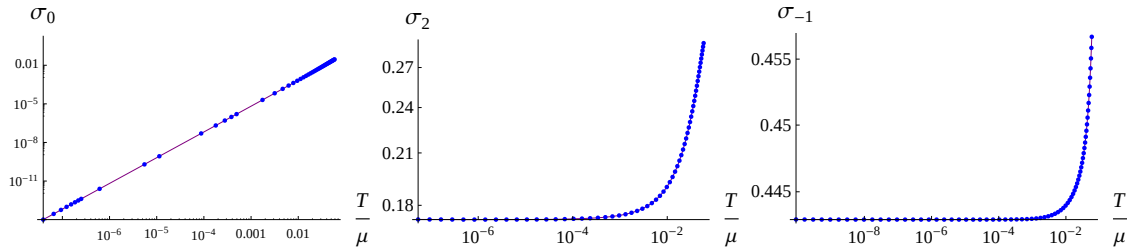

Figure 8: The coefficients σ_0, σ_2 and σ_{-1}. The plot has been truncated for σ_0 and σ_2 for very low temperatues, as $\mathrm{Re}\,\sigma$ became numerically indistinguishable from zero and a fit could not be done.

conductivity as

$$\mathrm{Re}\,\sigma \sim \sigma_0 + \sigma_2 \left(\frac{\omega}{\mu}\right)^2, \qquad \mathrm{Im}\,\sigma \sim \sigma_{-1}\frac{\mu}{\omega} \tag{4.9}$$

for small ω, it can seen that σ_2 and σ_{-1} level off for small temperatures and σ_0 decreases like a power law in T in this limit. This is consistent with the result in [5], where σ_0 is not present. Above the critical temperature the background is an AdS-RN black brane and the calculation of the conductivity reduces to the one described in [2].

5. Discussion

One of the most interesting recent developments in holographic model building is the observation that at low temperatures it can be energetically favorable for black holes in AdS space to eject their charge in the form of matter "hair" [7, 16, 17, 18, 19]. In the boundary theory this hair may give rise to many interesting features including spontaneous symmetry breaking [20], dynamical critical exponents [5] and non-fermi liquids [7, 21]. In general, this may allow one to use holographic techniques to study condensed matter systems not amenable to other theoretical tools.

In this paper we explored the finite boundary temperature generalization of the electron star configuration described in [5]. The electron star solution is a zero temperature model for a quantum phase transition displaying dynamical critical exponents as well as non-fermi liquid features. In the bulk the configuration is that of a zero temperature ideal charged fermion fluid. In the deep interior this fluid has an asymptotic Lifshitz scaling symmetry. As one approaches the boundary, the gauge potential is screened by the charged fluid. Eventually, the local chemical potential falls below the fermion mass causing the fluid density to vanish. In the asymptotic region one is left with an AdS-RN geometry.

At finite boundary temperatures there is instead a cloud-like configuration, with the electron fluid hovering outside an AdS-RN black brane geometry. This configuration is only possible when the fluid and black brane have same sign charges such

that electrostatic repulsion balances gravitational attraction. Within the fluid and its exterior, the electron cloud solution is similar to the electron star. The gauge field is screened and eventually the fluid can no longer be supported. We found that as one lowers the temperature, for fixed chemical potential one smoothly obtains the free energy of the electron star solution at zero temperature.

In the other extreme, beyond a critical temperature the local chemical potential is always lower than the fermion mass and no fermion fluid is supported. In this case we are left with an AdS-RN black brane geometry. We studied the transition numerically and found that it is a third order phase transition, as pointed out in [10].

We can summarize the phase diagram as follows, in the high temperature regime there is an AdS-RN black brane. As one lowers the temperature it is favorable for the black brane to expel some of its charge in the form of an electron cloud hovering over the horizon. As one cools the system further, the interior black brane carries less and less charge and has shrinking area. Finally, at zero temperature the black brane is gone and the fluid takes the form of an electron star.

In addition to studying electron cloud thermodynamics we also computed the conductivity, finding that it is nicely consistent with the electron star results of [5] at low temperature and with the AdS-RN black brane at high temperature.

In [21] it was argued that if the fluid in an electron star experiences a local temperature and magnetic field, it is possible to detect a Fermi surface evidenced by Kosevich-Lifshitz oscillations. It should also be possible to see such oscillations in electron clouds.

A major challenge for the construction we are working with is how to interpret the electron fluid directly in terms of operators in the boundary field theory. It would be interesting to see how the work of [8] may be extended for charged fluids in order to further characterize the nature of the underlying quantum critical point.

Acknowledgments

We thank S. A. Hartnoll and K. Schalm for helpful discussions. This work was supported in part by the Icelandic Research Fund and by the University of Iceland Research Fund.

References

[1] C. P. Herzog, "Lectures on Holographic Superfluidity and Superconductivity," J. Phys. A: Math. Theor. **42** 2009 343001 [arXiv:0904.1975 [hep-th]].

[2] S. A. Hartnoll, "Lectures on holographic methods for condensed matter physics," Class. Quant. Grav. **26**, 224002 (2009) [arXiv:0903.3246 [hep-th]].

[3] J. McGreevy, "Holographic duality with a view toward many-body physics," Adv. High Energy Phys. **2010**, 723105 (2010) [arXiv:0909.0518 [hep-th]].

[4] S. Sachdev, 'Strange metals and the AdS/CFT correspondence," J. Stat. Mech. **1011**, P11022 (2011) [arXiv:1010.0682 [cond-mat.str-el]].

[5] S. A. Hartnoll and A. Tavanfar, "Electron stars for holographic metallic criticality," arXiv:1008.2828 [hep-th].

[6] J. de Boer, K. Papadodimas, E. Verlinde, "Holographic Neutron Stars," JHEP **1010** (2010) 020 [arXiv:0907.2695 [hep-th]].

[7] S. A. Hartnoll, J. Polchinski, E. Silverstein and D. Tong, "Towards strange metallic holography," JHEP **1004** (2010) 120 [arXiv:0912.1061 [hep-th]].

[8] X. Arsiwalla, J. de Boer, K. Papadodimas *et al.*, "Degenerate Stars and Gravitational Collapse in AdS/CFT," [arXiv:1010.5784 [hep-th]].

[9] V. Parente and R. Roychowdhury, "A Study on Charged Neutron Star in AdS_5," arXiv:1011.5362 [hep-th].

[10] S. A. Hartnoll and P. Petrov, "Electron star birth: A continuous phase transition at nonzero density," [arXiv:1011.6469 [hep-th]].

[11] E. Gubankova, J. Brill, M. Cubrovic, K. Schalm, P. Schijven and J. Zaanen, "Holographic fermions in external magnetic fields," [arXiv:1011.4051 [hep-th]].

[12] G. W. Gibbons and S. W. Hawking, "Action Integrals And Partition Functions In Quantum Gravity," Phys. Rev. D **15**, 2752 (1977).

[13] M. Henningson and K. Skenderis, "The holographic Weyl anomaly," JHEP **9807**, 023 (1998) [arXiv:hep-th/9806087].

[14] V. Balasubramanian and P. Kraus, "A stress tensor for anti-de Sitter gravity," Commun. Math. Phys. **208**, 413 (1999) [arXiv:hep-th/9902121].

[15] D. T. Son and A. O. Starinets, "Minkowski-space correlators in AdS/CFT correspondence: Recipe and applications," JHEP **0209**, 042 (2002) [arXiv:hep-th/0205051].

[16] S. A. Hartnoll, C. P. Herzog, G. T. Horowitz, "Holographic Superconductors," JHEP **0812** (2008) 015 [arXiv:0810.1563 [hep-th]].

[17] S. S. Gubser, A. Nellore, "Low-temperature behavior of the Abelian Higgs model in anti-de Sitter space," JHEP **0904** (2009) 008 [arXiv:0810.4554 [hep-th]].

[18] G. T. Horowitz, M. M. Roberts, "Zero Temperature Limit of Holographic Superconductors," JHEP **0911** (2009) 015 [arXiv:0908.3677 [hep-th]].

[19] J. P. Gauntlett, J. Sonner and T. Wiseman, "Holographic superconductivity in M-Theory," Phys. Rev. Lett. **103** (2009) 151601 [arXiv:0907.3796 [hep-th]].

[20] S. S. Gubser, "Breaking an Abelian gauge symmetry near a black hole horizon," Phys. Rev. **D78** (2008) 065034 [arXiv:0801.2977 [hep-th]].

[21] S. A. Hartnoll, D. M. Hofman, A. Tavanfar, "Holographically smeared Fermi surface: Quantum oscillations and Luttinger count in electron stars," [arXiv:1011.2502 [hep-th]].